DEVELOPMENT OF TOMOGRAPHIC RECONSTRUCTION METHODS FOR STUDIES OF TRANSVERSE PHASE SPACE IN THE EMMA FFAG INJECTION LINE*

M. G. Ibison#, K. M. Hock, D. J. Holder and M. Korostelev
University of Liverpool and the Cockcroft Institute, UK

Abstract

We present a simulation study on the reconstruction of the phase space distribution of a beam in the EMMA injection line. The initial step has been to use a Gaussian beam to calculate the phase space distribution and the horizontal and vertical beam projections which would be expected at a screen. The projections obtained from a range of optical configurations are provided as input for reconstructing the phase space distribution using a standard tomography method. The result from the reconstruction can be compared with the known phase space distribution. By taking into account the limited range of quadrupole strengths available, we can determine how practical limitations may affect the reconstruction.

INTRODUCTION

The EMMA non-scaling Fixed-Field Alternating-Gradient (FFAG) accelerator is currently being constructed at the STFC Daresbury Laboratory, UK [1]. One key beam diagnostic that will be needed is the characterisation of transverse phase space before and after acceleration, so that the effects of space charge, decoherence and other phenomena may be studied. For this purpose, phase space tomography sections have been included in the injection and extraction lines of EMMA [2, 3].

We report here the results of a simulation study on the reconstruction of the phase space distribution in the injection line. The beamline is described, followed by a brief review of the tomography reconstruction method used. The method of simulating and reconstructing the electron beam is then explained, and the effect of limitations in the available range of quadrupole strengths is discussed.

EMMA INJECTION LINE

The layout of part of the EMMA injection line is shown in Fig. 1. The tomography section consists of two FODO cells, each with Yttrium Aluminium Garnet (YAG) screens at either end. Immediately before the tomography section is a matching section of four quadrupole magnets. Each quadrupole has a magnetic length of 0.07 m, and a maximum gradient of 14.7 T/m, corresponding to a current of 10 A.

The design of the injection line, and of the tomography section in particular, is based on collection of tomography data at the three screens, with the quadrupole strengths fixed for a betatron phase advance of 60° from one screen to the next. In this study, we investigate the possibility of improving the measurement of the phase space distribution by adjusting the quadrupole strengths (and therefore the betatron phase advance between the screens) to provide additional data points.

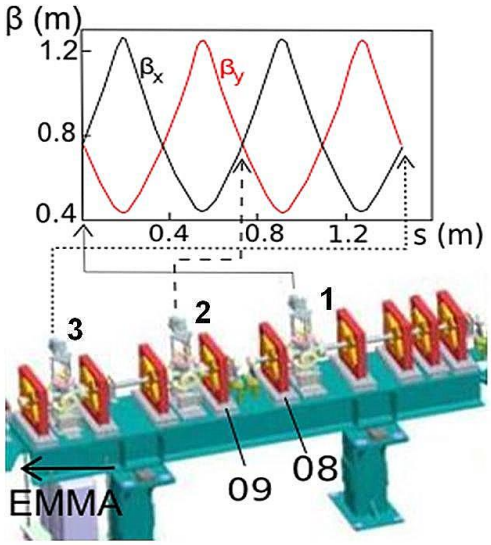

Figure 1: Matching and tomography sections of the injection line to EMMA, showing design β-functions at the three screens.

Our simulation is associated with the screens labelled '1', '2' and '3', and the quadrupoles labelled '08' and '09' in Fig. 1. The electron beam properties have been modelled in [2, 3]. From recent measurements using the 'slit-scan' technique [4], the emittance is known to be in the range of 5 to 10 mm.mrad.

SIMULATION METHOD

The principle behind tomography measurements can be understood in terms of transformations in phase space. The coordinate space distribution observed on Screen 3 (Fig. 1) depends on the initial phase space distribution (i.e. the distribution just before Screen 1), and on the strengths of the quadrupoles and lengths of the drifts between Screens 1 and 3. By setting the quadrupole strengths to a range of known values and observing the corresponding coordinate space distributions on Screen 3, the initial phase space distribution can be determined. By carrying out simulations starting with known initial phase

*Work supported by the Science & Technology Facilities Council, UK.
#mark.ibison@stfc.ac.uk

space distributions, the accuracy of the reconstruction, and its dependence on various parameters (such as the number and range of quadrupole strengths used) can be explored.

In the simulation, we consider for now only the horizontal (x direction) phase space. From the initial phase space distribution, we calculate the distribution at the screen. Assuming purely linear dynamics (that is, ignoring nonlinear effects that may arise from large oscillation amplitudes and space charge) and assuming a Gaussian initial phase space distribution, the projection on Screen 3 can be calculated analytically for given strengths of the quadrupoles. More generally, the projection may be obtained from a tracking simulation.

The reconstruction is then carried out using a standard method [5]. The procedure consists of three main steps:

1. Finding the angle of the projection.
2. Scaling the intervals for the projection.
3. Scaling the projection itself.

The angle of projection may be understood in terms of transformations in phase space. Fig. 2 shows an initial square distribution in phase space, that becomes 'sheared' as the beam passes through a drift space before hitting a screen. The particles between lines A and B in the sheared phase space are contained between lines A' and B' in the original phase space: the number of particles between these lines is observed from the intensity distribution on the screen (the 'projected distribution'). The angle of projection is the angle that lines A' and B' make with the x-axis in the original phase space. By varying this angle of projection, (in this example, changing the length of the drift space) and observing the corresponding intensity distribution on the screen, the original phase space distribution may be reconstructed.

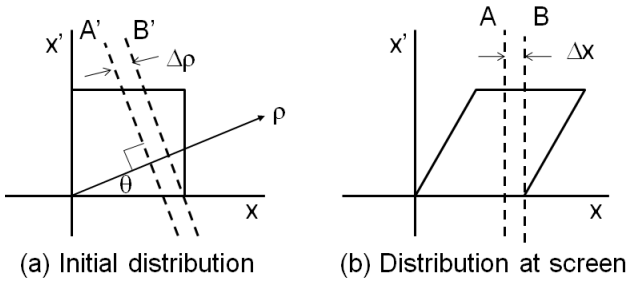

Figure 2: (a) Schematic phase space distribution just before the quadrupole. (b) Reconstructed phase space.

In general, a linear transformation in one degree of freedom along a beamline can be written as a transfer matrix:

$$M = \begin{pmatrix} R_{11} & R_{12} \\ R_{21} & R_{22} \end{pmatrix}. \qquad (1)$$

In terms of the transfer matrix from the location of the initial distribution to the location of the observation screen, the angle of projection (step 1 above) is given by:

$$\tan\theta = \frac{R_{12}}{R_{11}}. \qquad (2)$$

Next (step 2), we need the interval $\Delta\rho$ in Fig. 2(a). This is related to the interval Δx in Fig. 2(b) by a scale factor given by:

$$s = \sqrt{R_{11}^2 + R_{12}^2}\ . \qquad (3)$$

The formula for the interval is:

$$\Delta\rho = \frac{\Delta x}{s}. \qquad (4)$$

Finally (step 3), suppose that the projection obtained in Fig. 2(b) is $p(x)$. The corresponding projection in Fig. 2(a) is given by:

$$f(\rho, \theta) = s\, p(x). \qquad (5)$$

The images recorded at the screen can thus be processed to give the projections at the initial distribution $f(\rho, \theta)$ for a range of ρ and θ. The image can then be reconstructed from the complete projection set (or 'sinogram') using a standard method for real space tomography [6]. We have written a Matlab code using the Filtered Back Projection (FBP) method for this purpose.

RESULTS AND DISCUSSION

We ran the simulation for the following cases:

i) Using the projected distributions at Screens 1, 2 and 3, and the nominal betatron phase advance of 60° between each screen and the next, the phase space distribution at Screen 1 was reconstructed. Note that the projection angles in this case are 0°, -48.5° and -22.3°. This represents the 'design' case.

ii) Taking projected distributions at a set of distances downstream from Screen 1, without any intervening quadrupoles, the phase space distribution at Screen 1 was reconstructed. The distances were chosen to give projection angles from -85° to +85°, in steps of 10°. This represents a hypothetical situation in which the quadrupoles in the tomography section are removed, and a number of additional screens inserted.

iii) Taking projected distributions at Screen 2 with Quad 09 turned off, and Quad 08 varied to give different projection angles, the phase space distribution at the entrance of Quad 08 was reconstructed. If the limit on the strength of Quad 08 is taken into account, this represents a practical situation.

In each case, the original phase space distribution is assumed to have a Gaussian profile with an emittance of 5 mm.mrad. The four matching quadrupoles upstream of Screen 1 were not adjusted at any point, so the lattice functions up to Screen 1 maintained their nominal values.

The initial phase space distribution and the reconstructed distribution for Case (i) are shown in Fig. 3. In this case, projected images at the three screens are recorded, without any adjustment of the optics. There are therefore only three projection angles: although some features of the original distribution are qualitatively reproduced, there are significant differences between the actual and reconstructed phase space distributions.

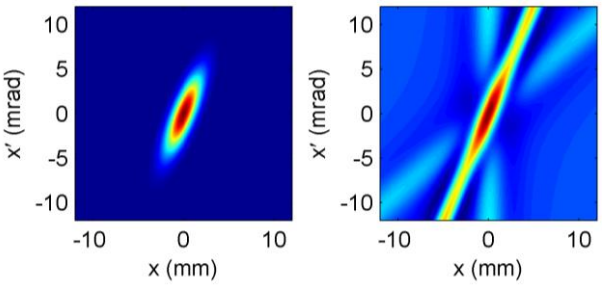

Figure 3: Original (left) and reconstructed (right) phase space distributions for Case (i).

For Case (ii) the reconstructed phase space distribution is shown in Fig. 4. Note that the original phase space distribution is the same as shown in Fig. 3. The reconstruction is clearly much closer to the original distribution than was the case for Case (i): this is because of the larger number of projections available. However, Case (ii) is somewhat idealised, since we assume that we can cover almost the full range of projection angles, using a set of screens that are not actually available in practice.

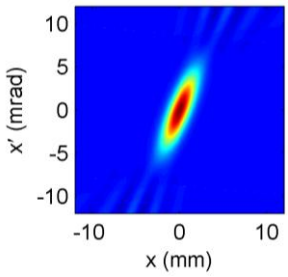

Figure 4: Phase space distribution reconstructed from varying drift lengths, Case (ii).

A more realistic situation is represented by Case (iii). In this case, we take projected images from Screen 2, and change the projection angle by adjusting the strength of Quad 08 up to the practical limit. The projection angles are computed from the transfer matrices (with given quadrupole strengths) using Eq. (2). The relationship between Quad 08 strength and the projection angle is shown in Fig. 5. Notice that the range of projection angles accessible is in the range 29° to 178° (less than 180°).

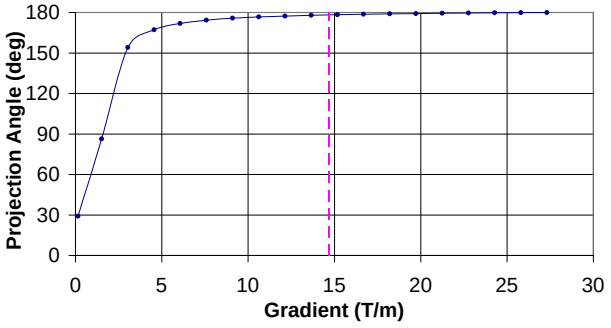

Figure 5: Accessible projection angles for Case (iii). The dashed line indicates the strength limit on Quad 08.

The reconstructed phase space distribution for Case (iii) is close to the original distribution (see Fig. 6). There is some limitation on the accuracy of the reconstruction from the limits on the range of projection angles that are accessible; however, it is again seen that a larger number of projection angles leads to a better reconstruction than for Case (i).

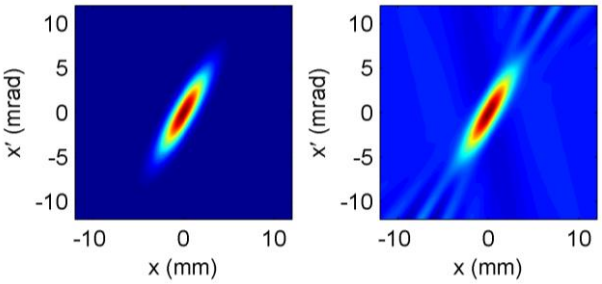

Figure 6: Original (left) and reconstructed (right) phase space distributions for Case (iii).

CONCLUSION

We have developed computer codes for modelling phase space tomography in the EMMA injection line. The simulations validate the codes that will be used for reconstructing the phase space distribution from the coordinate space distributions observed on YAG screens. Using the codes, we can study different procedures for data collection and analysis, and determine, for example, an appropriate range and number of quadrupole settings to be used for data collection. With further development, the codes will allow us to simulate and study the effects of practical issues such as fluctuations in beam intensity, beam positions, camera resolution, space charge, etc.

The authors would like thank Bruno Muratori (STFC/ASTeC) for his invaluable support throughout this work, and Andy Wolski (University of Liverpool) for his kind assistance with drafting the paper.

REFERENCES

[1] R. Edgecock *et al*, "EMMA: The World's First Non-Scaling FFAG," Proceedings of EPAC'08, Genoa, Italy.

[2] B.D. Muratori *et al*, "Injection and Extraction for the EMMA NS-FFAG", EPAC'08, Genoa, Italy.

[3] D.J. Holder and B.D. Muratori, "Modelling the ALICE electron beam properties through the EMMA Injection Line Tomography Section," Proceedings of PAC'09, Vancouver, Canada.

[4] J. Garland, "Characterisation and Optimisation of the ALICE Accelerator as an Injector for the EMMA NS-FFAG", Proceedings of IPAC'10, Kyoto, Japan.

[5] C.B. McKee, P.G. O'Shea, J.M.J. Madey, Nuclear Instruments and Methods in Physics Research A 358 (1995) 764.

[6] A. C. Kak and M. Slaney, "Principles of Computerized Tomographic Imaging", (SIAM, Philadelphia, USA, 2001), pp. 60-75.